Available online at www.sciencedirect.com
ScienceDirect
Journal of Sound and Vibration 321 (2009) 166–183
JOURNAL OF SOUND AND VIBRATION
www.elsevier.com/locate/jsvi

Vibration analysis of bimodulus laminated cylindrical panels

K. Khan, B.P. Patel*, Y. Nath

Department of Applied Mechanics, Indian Institute of Technology Delhi, Hauz Khas, New Delhi 110016, India

Received 12 July 2008; received in revised form 24 August 2008; accepted 11 September 2008
Handling Editor: J. Lam
Available online 23 October 2008

Abstract

This paper deals with the flexural vibration behavior of bimodular laminated composite cylindrical panels with various boundary conditions. The formulation is based on first order shear deformation theory and Bert's constitutive model. The governing equations are derived using finite element method and Lagrange's equation of motion. An iterative eigenvalue approach is employed to obtain the positive and negative half cycle free vibration frequencies and corresponding mode shapes. A detailed parametric study is carried out to study the influences of thickness ratio, aspect ratio, lamination scheme, edge conditions and bimodularity ratio on the free vibration characteristics of bimodulus angle- and cross-ply composite laminated cylindrical panels. It is interesting to observe that there is a significant difference between the frequencies of positive and negative half cycles depending on the panel parameters. Through the thickness distribution of modal stresses for positive half cycle is significantly different from that for negative half cycle unlike unimodular case wherein the stresses at a particular location in negative half cycle would be of same magnitude but of opposite sign of those corresponding to positive half cycle. Finally, the effect of bimodularity on the steady state response versus forcing frequency relation is studied for a typical case.

1. Introduction

Generally, the composite structures are analyzed considering material as unimodular i.e. material properties are assumed to be same in tension and compression. But there are certain fiber reinforced composites which exhibit different properties in tension and compression. Their actual stress–strain relation is often approximated by two straight lines with a slope discontinuity at origin (Refer Fig. 1). Most commonly used composites exhibiting bimodularity are: unidirectional glass/epoxy composites with compression moduli 20% smaller than the tension moduli, boron/epoxy laminates having compression moduli about 15–20% greater than the tension moduli and graphite/epoxy laminates with tension moduli up to 40% greater than the compression moduli [1,2]. Analysis of structures made of such materials based on bimodular approach is more appropriate. The fiber direction strain governed symmetric compliance bimodulus material model proposed by Bert [3] is commonly employed.

*Corresponding author. Tel.: +91 011 26591232; fax: +91 011 26581119.
E-mail address: badripatel@hotmail.com (B.P. Patel).

0022-460X/$ - see front matter
doi:10.1016/j.jsv.2008.09.017

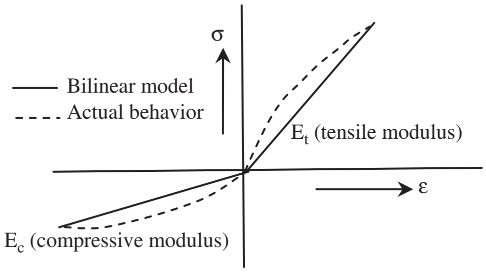

Fig. 1. Approximation of actual stress–strain behavior with bilinear model.

Few studies [4–9] have been carried out on the dynamic analysis of bimodular material laminated plates/shells. The free vibration analysis of two-layered cross-ply bimodulus composite simply supported thick rectangular plates has been carried out by Bert et al. [4]. The effect of pure bending and extensional pre-stresses on the free flexural vibration frequencies of simply supported thick bimodulus orthotropic plates has been studied by Doong and Chen [5]. The vibration and buckling analyses of simply supported orthotropic and two-layered cross-ply rectangular plates of bimodular material have been carried out using finite element approach based on higher order shear deformation theory by Doong and Fung [6]. The free flexural vibration analysis of bimodular laminated angle-ply plates has been carried out using finite element approach based on higher order shear deformation theory [7]. The dynamic stability analysis of bimodular isotropic rectangular plate subjected to periodic in-plane load has been carried out using finite element method based on first order shear deformation theory by Jzeng et al. [8]. The free vibration study of two-layered cross-ply simply supported cylindrical panels of bimodulus material has been carried out by Bert and Kumar [9]. The above cited studies are specific to mostly isotropic/orthotropic/two-layered cross-ply laminated bimodular plates/panels with all edges simply supported.

To the best of the authors' knowledge, the effect of different support conditions and number of layers on the vibration characteristics of cross- and angle-ply laminated cylindrical panels of bimodulus material is not dealt in the open literature.

In this paper, the vibration analysis of cross- and angle-ply bimodular material laminated cylindrical panels with various edge conditions (all edges simply supported (SSSS), all edges clamped (CCCC), straight edges simply supported and curved edges clamped (SCSC), straight edges clamped and curved edges simply supported (CSCS)) is carried out using finite element method. The effect of aspect ratio, ply-angle, number of layers (all the layers are of equal thickness) and bimodularity ratios (E_{2t}/E_{2c}) on the free vibration characteristics of cylindrical panels is investigated. The non-dimensional positive and negative half cycle frequencies and modal stress distributions are presented. The effect of bimodularity on the steady state response versus forcing frequency relation is shown for a typical case.

2. Constitutive model

Based on the fiber direction strain governed model, the constitutive relation of a bimodulus laminated material can be written as [4]:

$$\{\sigma^k\} = \begin{Bmatrix} \sigma^k_{ss} \\ \sigma^k_{\theta\theta} \\ \tau^k_{s\theta} \\ \tau^k_{sz} \\ \tau^k_{\theta z} \end{Bmatrix} = \begin{bmatrix} \bar{Q}_{11kl} & \bar{Q}_{12kl} & \bar{Q}_{16kl} & 0 & 0 \\ \bar{Q}_{12kl} & \bar{Q}_{22kl} & \bar{Q}_{26kl} & 0 & 0 \\ \bar{Q}_{16kl} & \bar{Q}_{26kl} & \bar{Q}_{66kl} & 0 & 0 \\ 0 & 0 & 0 & \bar{Q}_{44kl} & \bar{Q}_{45kl} \\ 0 & 0 & 0 & \bar{Q}_{45kl} & \bar{Q}_{55kl} \end{bmatrix} \begin{Bmatrix} \varepsilon_{ss} \\ \varepsilon_{\theta\theta} \\ \gamma_{s\theta} \\ \gamma_{sz} \\ \gamma_{\theta z} \end{Bmatrix} = [\bar{Q}_{ijkl}]\{\varepsilon\} \tag{1}$$

where $\bar{Q}_{ijkl}$ are transformed stiffness coefficients and k is layer number, $l = 1$ denotes the properties associated with fiber direction tension and $l = 2$ denotes the properties associated with fiber direction compression.

3. Governing equations

A bimodular material laminated composite cylindrical panel is considered as shown in Fig. 2 with total thickness h, radius r, meridional length L and circumferential length b. The displacements u, v and w at a point (s, θ, z) from the median surface are expressed as functions of middle surface displacements u_0,v_0,w_0 and independent rotations β_s and β_θ of the meridional and hoop sections, respectively, as:

$$
\begin{aligned}
u\,(s,\ \theta,\ z,\ t) &= u_0\,(s,\ \theta,\ t)\ +\ z\,\beta_s\,(s,\ \theta,\ t)\\
v\,(s,\ \theta,\ z,\ t) &= v_0\,(s,\ \theta,\ t)\ +\ z\,\beta_\theta\,(s,\ \theta,\ t)\\
w\,(s,\ \theta,\ z,\ t) &= w_0\,(s,\ \theta,\ t)
\end{aligned}
\tag{2}
$$

The strain vector can be written as:

$$
\{\varepsilon\} = \begin{Bmatrix} \varepsilon_{ss} \\ \varepsilon_{\theta\theta} \\ \gamma_{s\theta} \\ \gamma_{sz} \\ \gamma_{\theta z} \end{Bmatrix} = \begin{Bmatrix} \varepsilon_p \\ 0 \end{Bmatrix} + \begin{Bmatrix} z\varepsilon_b \\ \varepsilon_s \end{Bmatrix}
\tag{3}
$$

The vectors $\{\varepsilon_p\}$, $\{\varepsilon_b\}$ and $\{\varepsilon_s\}$ represent mid-surface membrane, bending and transverse shear strains, respectively, and are defined as [10]:

$$
\{\varepsilon_p\} = \begin{Bmatrix} \dfrac{\partial u_0}{\partial s} \\ \dfrac{\partial v_0}{r\partial\theta} + \dfrac{w_0}{r} \\ \dfrac{\partial u_0}{r\partial\theta} + \dfrac{\partial v_0}{\partial s} \end{Bmatrix}, \quad \{\varepsilon_b\} = \begin{Bmatrix} \dfrac{\partial\beta_s}{\partial s} \\ \dfrac{\partial\beta_\theta}{r\partial\theta} \\ \dfrac{\partial\beta_s}{r\partial\theta} + \dfrac{\partial\beta_\theta}{\partial s} \end{Bmatrix}, \quad \{\varepsilon_s\} = \begin{Bmatrix} \beta_s + \dfrac{\partial w_0}{\partial s} \\ \beta_\theta + \dfrac{\partial w_0}{r\partial\theta} - \dfrac{v_0}{r} \end{Bmatrix}
\tag{4}
$$

The kinetic energy of the shell is expressed as:

$$
T(\delta) = \frac{1}{2}\int\int\left[\sum_{k=1}^{N}\int_{h_k}^{h_{k+1}} \rho_k\{\dot{u}_k\ \dot{v}_k\ \dot{w}_k\}\{\dot{u}_k\ \dot{v}_k\ \dot{w}_k\}^{\mathrm{T}}\,\mathrm{d}z\right] r\,\mathrm{d}s\,\mathrm{d}\theta
\tag{5}
$$

where ρ_k is the mass density of the kth layer, h_k, h_{k+1} are the z-coordinates of the bottom and top surfaces of the kth layer and $\{\delta\} = \{\delta_1, \delta_2, \ldots\ldots\ldots, \delta_n\}$ is the vector of degrees of freedom.

Using Eq. (2), Eq. (5) can be rewritten as:

$$
T(\delta) = \frac{1}{2}\int\int\left[\sum_{k=1}^{N}\int_{h_k}^{h_{k+1}} \rho_k\{\dot{d}^e\}^{\mathrm{T}}[Z]^{\mathrm{T}}[Z]\{\dot{d}^e\}\,\mathrm{d}z\right] r\,\mathrm{d}s\,\mathrm{d}\theta
\tag{6}
$$

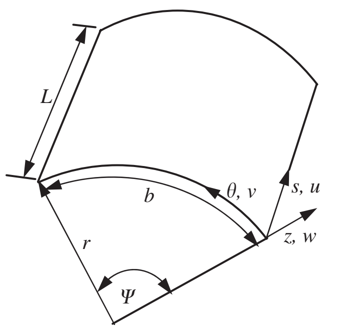

Fig. 2. Geometry and coordinate system of cylindrical panel.

where

$$\{\dot{d}^e\}^{\mathrm{T}} = \{\dot{u}_0\ \dot{v}_0\ \dot{w}_0\ \dot{\beta}_s\ \dot{\beta}_\theta\} \quad \text{and} \quad [Z] = \begin{bmatrix} 1 & 0 & 0 & z & 0 \\ 0 & 1 & 0 & 0 & z \\ 0 & 0 & 1 & 0 & 0 \end{bmatrix}$$

The potential energy of the shell is given by:

$$U(\delta) = \frac{1}{2}\int\int\left[\sum_{k=1}^{N}\int_{h_k}^{h_{k+1}}\{\sigma\}^{\mathrm{T}}\{\varepsilon\}\,\mathrm{d}z\right] r\,\mathrm{d}s\,\mathrm{d}\theta - \int\int q\,w_0\,r\,\mathrm{d}s\,\mathrm{d}\theta \tag{7}$$

where q is distributed force.

Using Eq. (1), Eq. (7) can be rewritten as:

$$U(\delta) = \frac{1}{2}\int\int\left[\sum_{k=1}^{N}\int_{h_k}^{h_{k+1}}\{\varepsilon\}^{\mathrm{T}}[\bar{Q}_{ijkl}]\,\{\varepsilon\}\,\mathrm{d}z\right] r\,\mathrm{d}s\,\mathrm{d}\theta - \int\int q\,w_0\,r\,\mathrm{d}s\,\mathrm{d}\theta \tag{8}$$

Analysis is carried out using a C^0 eight-noded serendipity quadrilateral shear flexible shell element with 5 degrees of freedom (u_0 ,v_0 , w_0 , β_s, β_θ) developed based on the field consistency approach [11]. The field variables are expressed in terms of nodal values using shape functions as:

$$(u_0,\ v_0,\ w_0,\ \beta_s,\ \beta_\theta) = \sum_{i=1}^{8} N_i^0\left(u_{0i},\ v_{0i},\ w_{0i},\ \beta_{si},\ \beta_{\theta i}\right) \tag{9}$$

where N_i^0 are the original shape functions for the eight-noded quadratic serendipity element. If the shape functions for an eight-noded element are used directly to interpolate the five field variables ($u_{0,}$ $v_{0,}$ $w_{0,}$ β_s, β_θ) in deriving the transverse shear strains for very thin shell, the element will lock and show oscillations in the transverse shear stresses. Field consistency requires that the transverse shear strains must be interpolated in a consistent manner [11]. This is achieved here by smoothing the original shape functions by least-square method to the desired form, i.e. the functions that are consistent with the derivative functions (${N^0}_{i,s}$ or ${N^0}_{i,\theta}$). The smoothened shape function ${N^1}_{si}$ and ${N^1}_{\theta i}$ consistent with derivative functions $w_{0,s}$ and $w_{0,\theta}$ are required for the interpolation of β_s and β_θ to be substituted in the expressions for the transverse shear strain components. Using the smoothed shape functions, the constrained transverse shear strain components are expressed as:

$$(\beta_s + w_{0,s}) = \sum_{i=1}^{8}(N_{si}^1\beta_{si} + N_{i,s}^0 w_{0i}) \tag{10}$$

$$\left(\beta_\theta + \frac{1}{r}w_{0,\theta} - \frac{v_0}{r}\right) = \sum_{i=1}^{8}\left(N_{\theta i}^1\beta_{\theta i} + \frac{1}{r}N_{i,\theta}^0 w_{0i} - \frac{N_{\theta i}^1}{r}v_{0i}\right) \tag{11}$$

The other strains are expressed in terms of original shape function (N_i^0) and their derivatives.

The governing equations of motion, considering dissipative forces, can be written as:

$$[M]\{\ddot{\delta}\} + [C]\{\dot{\delta}\} + [K]\{\delta\} = \{F\} \tag{12}$$

where $[M]$, $[K]$ and $[C]$ are global mass, stiffness and damping matrices and $\{F\}$ is consistent global load vector. Neglecting the dissipative forces and load vector and assuming solution $\{\delta\} = \{\bar{\delta}\}\mathrm{e}^{i\omega t}$ for free vibration analysis, Eq. (12) becomes:

$$[K]\{\bar{\delta}\} = \omega^2[M]\{\bar{\delta}\} \tag{13}$$

Free vibration frequencies and corresponding modal vectors are extracted using Lanczos eigenvalue extraction technique. Forced response analysis is carried out by integrating Eq. (12) using Newmark's direct time integration scheme.

4. Iterative eigenvalue approach

For the analysis of bimodular material laminated shells, it is necessary to determine the proper combination of material properties and strain in the fiber direction (ε_{11}). To start the iteration, all the layers are assigned tensile properties and eigenvalue problem (Eq. 13) is solved.

Then for the normalized mode shape of interest (number of half waves m along s-direction and n along θ-direction), the location of neutral surface is determined using the zero fiber direction strain condition for each layer. If the neutral surface is located inside a layer instead of at the interface between the two layers or outside the layer, the layer is split into two sub-layers. Then the tensile or compressive material properties are assigned to each layer depending upon the sign of the fiber direction strain (ε_{11}). Using the assigned properties, eigenvalue problem is solved. Again the mode shape of interest (m, n) is used to locate the neutral surface location for each layer. This process is repeated till frequencies and normalized mode shape from two consecutive iterations converge to a specified tolerance limit of 0.001%.

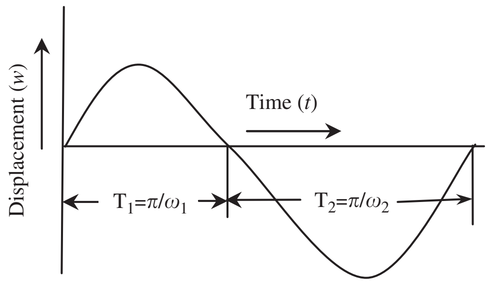

Fig. 3. Free vibration response during two portions of vibration cycle of a panel.

Table 1
(a) Comparison of non-dimensional frequencies (Ω_1, Ω_2) for different aspect (L/b) ratio of two-layered cross-ply (0°/90°) bimodular simply supported plate ($b/h = 10$, Material 1) and (b) comparison of non-dimensional frequency (Ω_1) for different aspect (L/b) and thickness (r/h) ratios of two-layered cross-ply bimodular simply supported cylindrical panel ($b/h = 10$, Material 1)

(a)

L/b	Ω_1		Ω_2	
	Ref. [4]	Present	Ref. [4]	Present
0.5	19.380	19.473	13.880	13.845
0.7	11.600	11.643	9.353	9.359
1.0	7.038	7.053	7.038	7.054
1.4	4.838	4.843	6.037	6.055
2.0	3.712	3.713	5.551	5.565

(b)

L/b	(90°/0°)				(0°/90°)			
	$r/h = 10$		$r/h = 50$		$r/h = 10$		$r/h = 50$	
	Ref. [9]	Present	Ref. [9]	Present	Ref. [9]	Present	Ref. [9]	Present
0.5	21.0200	22.0815	19.0463	19.4943	17.1875	17.4429	14.0244	14.2788
0.7	14.2052	14.3418	11.6098	11.8907	11.9665	12.0867	9.7942	9.7063
1.0	9.3674	9.3866	7.3443	7.3545	8.5365	8.6509	7.3932	7.2443
1.4	6.5556	6.5727	5.0287	5.0935	6.5167	6.6841	5.9070	6.1063
2.0	4.6281	4.7474	3.9409	3.8721	5.3353	5.4417	5.4115	5.5148

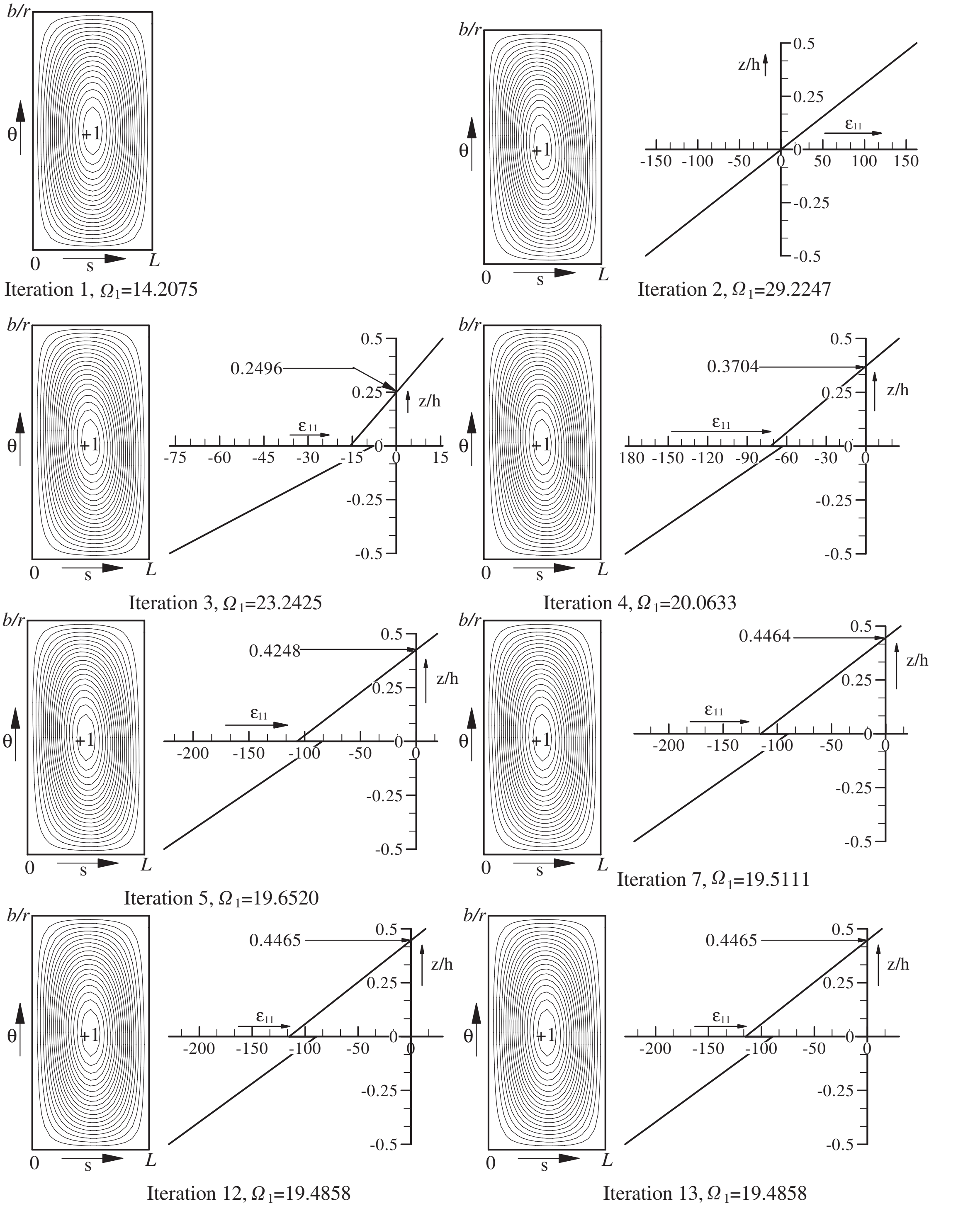

Fig. 4. Convergence study for mode shape and fiber direction strain distribution through the thickness for positive half cycle of two-layered angle-ply (15°/−15°) CSCS panel ($r/h = 50$, $b/h = 10$, $L/b = 0.5$, Material 1).

5. Results and discussion

Based on progressive mesh refinement, 10×10 mesh is found to be adequate to model the full panels. The material properties considered in the analysis are [9,12]:

Material 1 (Aramid-rubber):

Tension: $E_{1t} = 3.58\,\text{GPa}$, $E_{2t} = E_{3t} = 0.00909\,\text{GPa}$, $G_{12t} = G_{13t} = 0.0037\,\text{GPa}$, $G_{23t} = 0.0029\,\text{GPa}$, $\nu_{12t} = \nu_{23t} = \nu_{13t} = 0.416$.

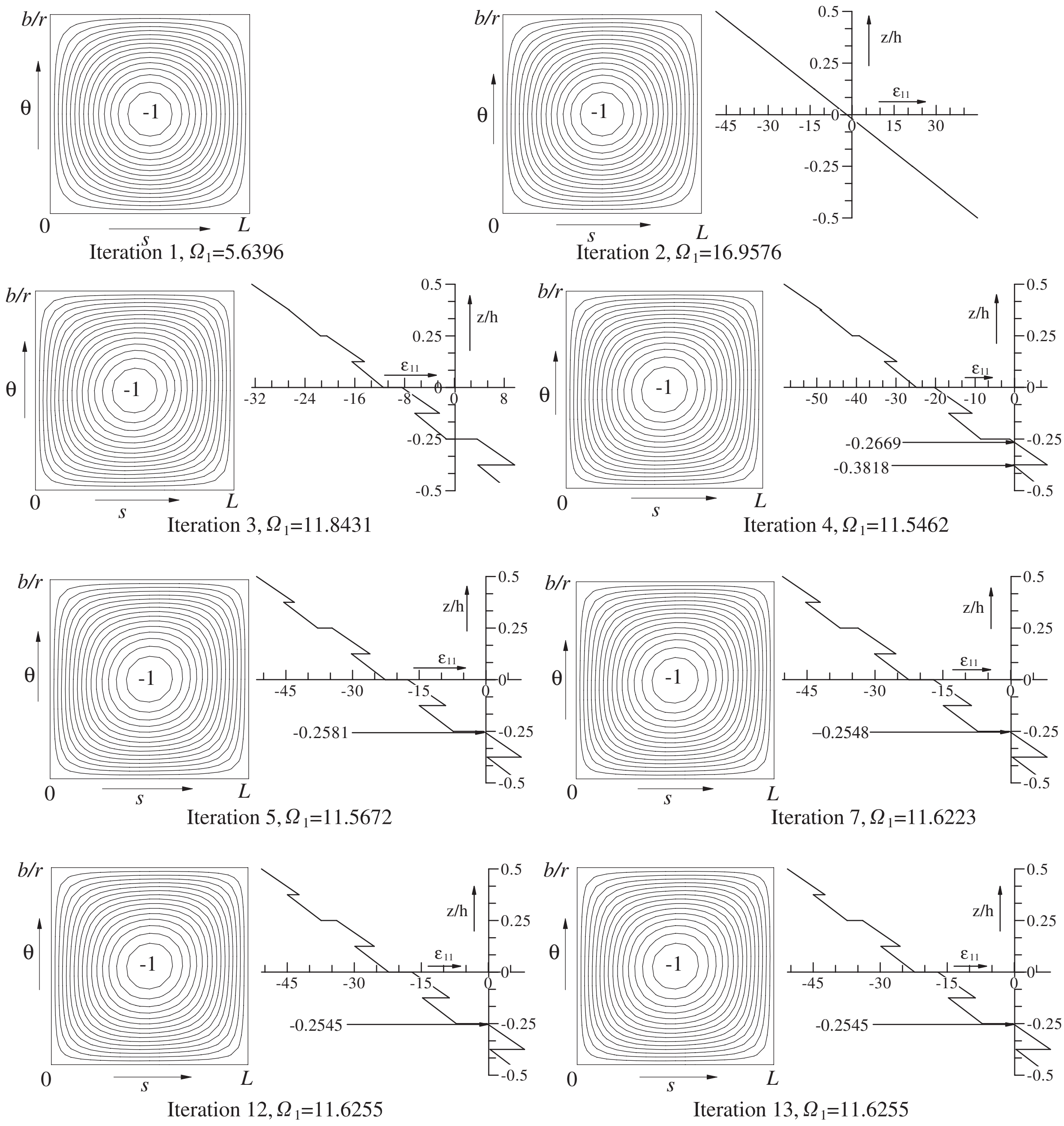

Fig. 5. Convergence study for mode shape and fiber direction strain distribution through the thickness for negative half cycle of eight-layered angle-ply $(45^\circ/-45^\circ)_4$ SSSS panel ($r/h = 100$, $b/h = 10$, $L/b = 1$, Material 1).

Compression: $E_{1c} = E_{2c} = E_{3c} = 0.012\,\text{GPa}$, $G_{12c} = G_{13c} = 0.0037\,\text{GPa}$, $G_{23c} = 0.00499\,\text{GPa}$, $\nu_{12c} = \nu_{23c} = \nu_{13c} = 0.205$.

Material 2:

Tension: $E_{1t}/E_{2t} = 25$, $E_{2t} = E_{3t}$, $G_{12t}/E_{2t} = G_{13t}/E_{2t} = 0.5$, $G_{23t}/E_{2t} = 0.2$, $\nu_{12t} = \nu_{23t} = \nu_{13t} = 0.25$.

Table 2
Non-dimensional positive and negative half cycle frequencies of angle-ply $(\theta/-\theta)_{N/2}$ bimodular laminated SSSS cylindrical panels ($b/h = 10$, Material 1)

L/b	θ	N	$r/h = 20$			$r/h = 50$			$r/h = 100$		
			Ω_1	Ω_2	% diff	Ω_1	Ω_2	% diff	Ω_1	Ω_2	% diff
0.5	15°	2	19.1102	18.6069	2.63	18.6728	18.4740	1.06	18.5819	18.4826	0.53
		4	19.2201	18.7908	2.23	18.7731	18.6082	0.87	18.6837	18.6036	0.42
		8	19.3742	19.1716	1.04	19.0025	18.9327	0.36	18.9408	18.9063	0.18
	30°	2	20.1072	18.9250	5.87	19.3887	18.9088	2.47	19.2154	18.9758	1.24
		4	20.4650	19.4657	4.88	19.7806	19.3741	2.05	19.6238	19.4212	1.03
		8	21.1839	20.3992	3.70	20.5981	20.2800	1.54	20.4677	20.3103	0.76
	45°	2	22.5739	19.0776	15.48	20.9869	19.5543	6.82	20.5485	19.8330	3.48
		4	23.6771	19.8664	16.09	22.0080	20.4349	7.14	21.5357	20.7496	3.65
		8	24.5064	20.9264	14.60	22.9256	21.4803	6.30	22.4907	21.7666	3.21
0.7	15°	2	12.3571	11.2829	8.69	11.6604	11.2363	3.63	11.4993	11.2878	1.83
		4	12.5731	11.4927	8.59	11.8143	11.3867	3.61	11.6429	11.4296	1.83
		8	12.6917	11.8135	6.91	12.0245	11.6794	2.87	11.8798	11.7069	1.45
	30°	2	14.0295	12.0606	14.03	12.9128	12.1043	6.26	12.6333	12.2268	3.21
		4	14.4914	12.6049	13.01	13.3587	12.5934	5.72	13.0844	12.6986	2.94
		8	14.9778	13.3102	11.13	13.9798	13.3004	4.85	13.7359	13.3949	2.48
	45°	2	17.8537	12.7877	28.37	15.3032	13.1788	13.88	14.6109	13.5383	7.34
		4	19.0957	13.4503	29.56	16.4957	14.1083	14.47	15.7597	14.5540	7.65
		8	19.3657	14.3494	25.90	17.1992	15.0020	12.77	16.5123	15.4095	6.67
1.0	15°	2	8.5777	6.9934	18.47	7.6679	7.0377	8.21	7.4464	7.1309	4.23
		4	8.9168	7.1831	19.44	7.8970	7.2046	8.76	7.6453	7.3000	4.51
		8	9.0002	7.4240	17.51	8.0661	7.4528	7.60	7.8444	7.5399	3.88
	30°	2	10.9645	7.9980	27.05	9.3733	8.1543	13.00	8.9602	8.3480	6.83
		4	11.5599	8.3831	27.48	9.8985	8.5818	13.30	9.4580	8.7956	7.00
		8	11.8291	8.8626	25.07	10.2948	9.1047	11.56	9.9024	9.3076	6.00
	45°	2	18.6919	8.9042	52.36	13.2380	9.3740	29.18	11.8448	9.9265	16.19
		4	19.6641	9.4242	52.07	14.1924	10.3515	27.06	12.8838	11.0228	14.44
		8	19.9468	10.1529	49.10	14.4914	11.0602	23.67	13.2523	11.6255	12.27
1.4	15°	2	6.7078	4.9366	26.40	5.7416	5.0545	11.96	5.5054	5.1648	6.18
		4	7.0678	5.0793	28.13	6.0049	5.2102	13.23	5.7306	5.3340	6.92
		8	7.1331	5.2471	26.44	6.1220	5.4025	11.75	5.8754	5.5198	6.05
	30°	2	10.0938	5.9064	41.48	7.9092	6.2214	21.33	7.3376	6.4889	11.56
		4	10.8980	6.1501	43.56	8.6303	6.6569	22.86	8.0068	7.0093	12.45
		8	11.1461	6.5104	41.59	8.8838	7.0695	20.42	8.2994	7.3961	10.88
	45°	2	9.0613	6.6882	26.18	8.1446	7.0948	12.88	7.8479	7.3136	6.80
		4	9.8482	7.1512	27.38	8.9591	7.7704	13.26	8.6469	8.0444	6.96
		8	10.2216	7.7390	24.28	9.4392	8.3627	11.40	9.1624	8.6147	5.97
2.0	15°	2	5.5321	3.8766	29.92	4.6501	4.0329	13.27	4.4360	4.1307	6.88
		4	5.8457	3.9659	32.15	4.8873	4.1534	15.01	4.6409	4.2740	7.90
		8	5.8932	4.0772	30.81	4.9485	4.2821	13.46	4.7232	4.3964	6.91
	30°	2	8.7661	4.6651	46.78	6.9499	5.1979	25.20	6.4109	5.5247	13.82
		4	9.5683	4.9284	48.49	7.7931	5.8038	25.52	7.2360	6.2291	13.91
		8	9.7993	5.2585	46.33	8.0496	6.1420	23.69	7.5146	6.5513	12.81
	45°	2	6.1176	5.4469	10.96	6.0054	5.7370	4.46	5.9526	5.8188	2.24
		4	6.5650	5.8093	11.51	6.4458	6.1431	4.69	6.3864	6.2361	2.35
		8	6.9384	6.2617	9.75	6.8637	6.5958	3.90	6.8163	6.6832	1.95

Compression: $E_{1c}/E_{2c} = 25$, $E_{2c} = E_{3c} = 1\,\text{GPa}$, $G_{12c}/E_{2c} = G_{13c}/E_{2c} = 0.5$, $G_{23c}/E_{2c} = 0.2$, $v_{12c} = v_{23c} = v_{13c} = 0.25$, E_{2t}/E_{2c} ratio is varied from 0.2 to 2.0.

Boundary conditions considered are:

Simply supported: $u_0 = w_0 = \beta_s = 0$ at $\theta = 0$ and b/r (straight edges), $v_0 = w_0 = \beta_\theta = 0$ at $s = 0$ and L (curved edges).

Clamped: $u_0 = v_0 = w_0 = \beta_s = \beta_\theta = 0$ at straight/curved edges.

Table 3
Non-dimensional positive and negative half cycle frequencies of angle-ply $(\theta/-\theta)_{N/2}$ bimodular laminated CSCS cylindrical panels ($b/h = 10$, Material 1)

L/b	θ	N	$r/h = 20$			$r/h = 50$			$r/h = 100$		
			Ω_1	Ω_2	% diff	Ω_1	Ω_2	% diff	Ω_1	Ω_2	% diff
0.5	15°	2	19.7833	20.0019	−1.10	19.4858	19.5813	−0.49	19.4574	19.5059	−0.24
		4	19.8506	20.0819	−1.16	19.5474	19.6445	−0.49	19.5184	19.5663	−0.24
		8	19.9798	20.4089	−2.14	19.7303	19.9065	−0.89	19.7140	19.8080	−0.47
	30°	2	20.6453	19.7617	4.27	20.0114	19.6526	1.79	19.8684	19.6883	0.90
		4	21.0253	20.2232	3.81	20.3940	20.0643	1.61	20.2563	20.0924	0.80
		8	21.7045	21.1107	2.73	21.1577	20.9134	1.15	21.0431	20.9207	0.58
	45°	2	22.8416	19.3810	15.15	21.2680	19.8468	6.68	20.8316	20.1214	3.40
		4	24.1360	20.2880	15.94	22.4637	20.8959	6.97	21.9939	21.2061	3.58
		8	25.0394	21.3574	14.70	23.4439	21.9593	6.33	23.0049	22.2595	3.24
0.7	15°	2	13.3459	13.4247	−0.59	12.8242	12.8616	−0.29	12.7542	12.7718	−0.13
		4	13.4742	13.5116	−0.27	12.9309	12.9481	−0.13	12.8525	12.8637	−0.08
		8	13.5964	13.7829	−1.37	13.1073	13.1860	−0.60	13.0424	13.0855	−0.33
	30°	2	14.9052	13.5218	9.28	13.9273	13.3445	4.18	13.6992	13.4043	2.15
		4	15.4874	13.9645	9.83	14.4612	13.8285	4.37	14.2175	13.9013	2.22
		8	16.0053	14.6227	8.63	15.0722	14.4900	3.86	14.8521	14.5564	1.99
	45°	2	18.6618	13.5788	27.23	16.1325	13.9933	13.26	15.4441	14.3666	6.97
		4	20.3398	14.4517	28.94	17.7142	15.2623	13.84	16.9744	15.7400	7.27
		8	21.1210	15.3579	27.28	18.5720	16.2053	12.74	17.8524	16.6679	6.63
1.0	15°	2	10.0279	9.9480	0.79	9.2649	9.2326	0.34	9.1460	9.1307	0.16
		4	10.2483	10.0424	2.00	9.4432	9.3529	0.95	9.3078	9.2618	0.49
		8	10.3867	10.2511	1.30	9.6145	9.5618	0.54	9.4918	9.4664	0.26
	30°	2	12.2731	10.2097	16.81	10.8581	9.9724	8.15	10.5168	10.0687	4.26
		4	13.1683	10.6354	19.23	11.6603	10.5787	9.27	11.2786	10.7305	4.85
		8	13.6584	11.1344	18.47	12.1897	11.1174	8.79	11.8151	11.2746	4.57
	45°	2	22.2692	10.4684	52.99	15.7691	11.0285	30.06	14.1012	11.7415	16.73
		4	23.5066	11.3320	51.79	17.3175	12.6531	26.93	15.7744	13.4940	14.45
		8	23.8879	12.1548	49.11	17.8671	13.5323	24.26	16.4305	14.3112	12.89
1.4	15°	2	8.6950	8.5102	2.12	7.7695	7.6831	1.11	7.6145	7.5704	0.57
		4	9.0400	8.5824	5.06	8.0365	7.8276	2.59	7.8502	7.7435	1.35
		8	9.1821	8.7503	4.70	8.2078	8.0203	2.28	8.0312	7.9367	1.17
	30°	2	11.9526	8.7741	26.59	9.8663	8.4818	14.03	9.3421	8.6413	7.50
		4	13.2295	9.2248	30.27	11.0665	9.3306	15.68	10.4883	9.6100	8.37
		8	13.7801	9.7036	29.58	11.6521	9.9319	14.76	11.0883	10.2232	7.80
	45°	2	25.5838	9.0474	64.63	17.6075	9.7706	44.50	14.7007	10.8685	26.06
		4	27.3083	9.8873	63.79	18.8066	11.6778	37.90	16.1365	12.8522	20.35
		8	27.9631	10.6746	61.82	19.1484	12.5396	34.51	16.5338	13.5989	17.75
2.0	15°	2	8.1419	7.8678	3.36	7.0951	6.9654	1.82	6.9113	6.8447	0.96
		4	8.6038	7.9276	7.85	7.4507	7.1388	4.18	7.2228	7.0632	2.20
		8	8.7208	8.0663	7.50	7.5954	7.3093	3.76	7.3799	7.2356	1.95
	30°	2	14.7262	8.0682	45.21	10.7041	7.8412	26.74	9.6357	8.1944	14.95
		4	15.7624	8.5891	45.50	12.0417	9.0520	24.82	11.0574	9.5574	13.56
		8	16.1768	9.1160	43.64	12.5138	9.7131	22.38	11.5838	10.1963	11.97
	45°	2	–	8.3255	–	18.4006	9.0466	50.83	15.0252	10.3588	31.05
		4	–	9.0946	–	19.5875	11.0764	43.45	16.3297	12.4351	23.84
		8	–	9.8417	–	19.8844	11.9267	40.01	16.6023	13.1535	20.77

The free vibration frequencies corresponding to positive and negative half cycles (Refer Fig. 3) are presented in the non-dimensional form as $(\Omega_1, \Omega_2) = (\omega_1, \omega_2)\, b^2(\rho/E_{2c}\, h^2)^{1/2}$ for mode with $(m, n) = (1, 1)$. The average frequency (ω) over the entire cycle is given by: $\omega = 2(1/\omega_1 + 1/\omega_2)^{-1}$. The formulation and computer program developed are validated against available solutions due to Bert et al. [4] and Bert and Kumar [9]. The results

Table 4
Non-dimensional positive and negative half cycle frequencies for angle-ply $(\theta/-\theta)_{N/2}$ bimodular laminated SCSC cylindrical panels ($b/h = 10$, Material 1)

L/b	θ	N	$r/h = 20$			$r/h = 50$			$r/h = 100$		
			Ω_1	Ω_2	% diff	Ω_1	Ω_2	% diff	Ω_1	Ω_2	% diff
0.5	15°	2	33.0949	31.5906	4.54	32.3058	31.7182	1.81	32.1183	31.8208	0.92
		4	33.9998	32.6040	4.10	33.2692	32.7149	1.66	33.0872	32.8099	0.83
		8	34.1620	32.9483	3.55	33.4959	33.0143	1.43	33.3343	33.0935	0.72
	30°	2	37.8017	30.0048	20.62	33.5793	31.0709	7.47	32.7805	31.5618	3.71
		4	38.3489	31.4845	17.89	34.1788	32.2852	5.54	33.5590	32.6537	2.69
		8	38.4109	32.0809	16.47	34.2730	32.7278	4.50	33.7333	33.0290	2.08
	45°	2	44.7225	26.9423	39.75	34.4209	28.9216	15.97	32.4550	29.8906	7.90
		4	45.7435	29.2530	36.04	35.2320	30.8863	12.33	33.3878	31.6200	5.29
		8	46.0565	30.2585	34.30	35.4105	31.6421	10.64	33.5876	32.2728	3.91
0.7	15°	2	24.1128	22.2904	7.55	23.1344	22.4093	3.13	22.8912	22.5292	1.58
		4	25.1353	23.3985	6.90	24.1959	23.5028	2.86	23.9631	23.6165	1.44
		8	25.3040	23.7764	6.03	24.4313	23.8319	2.45	24.2240	23.9248	1.23
	30°	2	29.7220	20.3383	31.57	24.7376	21.5920	12.71	23.7302	22.1972	6.46
		4	30.3944	22.1374	27.16	25.5505	23.1061	9.56	24.7366	23.5665	4.73
		8	30.5074	22.8327	25.15	25.6735	23.6204	7.99	24.9358	23.9937	3.77
	45°	2	33.4715	17.1650	48.71	24.5855	18.7615	23.68	22.5145	19.7323	12.35
		4	33.8296	19.2890	42.98	25.8132	21.0313	18.52	23.9685	21.8552	8.81
		8	35.0778	20.4069	41.82	26.1918	21.9043	16.36	24.4000	22.6104	7.33
1.0	15°	2	17.3835	15.3242	11.84	16.1905	15.3685	5.07	15.9026	15.4916	2.58
		4	18.4230	16.4636	10.63	17.2971	16.5083	4.56	17.0231	16.6267	2.32
		8	18.5653	16.8541	9.21	17.5082	16.8410	3.81	17.2661	16.9334	1.92
	30°	2	22.8606	13.2181	42.17	17.7510	14.2420	19.76	16.6025	14.8706	10.43
		4	23.7238	15.0291	36.64	18.7857	16.0124	14.76	17.8822	16.5297	7.56
		8	23.9016	15.8122	33.84	18.9776	16.6214	12.41	18.1351	17.0565	5.94
	45°	2	20.5665	11.1072	45.99	15.1148	11.4989	23.92	13.7839	12.0097	12.87
		4	21.6538	12.3241	43.08	16.6124	13.2200	20.42	15.4304	13.7979	10.57
		8	21.9939	13.2288	39.85	17.1551	14.1161	17.71	16.0841	14.6239	9.07
1.4	15°	2	12.8587	10.8238	15.82	11.5231	10.6970	7.16	11.2103	10.7931	3.72
		4	13.8739	11.9045	14.19	12.6496	11.8434	6.37	12.3548	11.9498	3.27
		8	14.0011	12.2826	12.27	12.8295	12.1670	5.16	12.5699	12.2412	2.61
	30°	2	16.6546	9.2076	44.71	12.3541	9.4855	23.21	11.3285	9.9062	12.55
		4	17.6371	10.5482	40.19	13.6612	11.1295	18.53	12.8093	11.5620	9.73
		8	17.8494	11.3024	36.67	13.9689	11.8017	15.51	13.1960	12.1552	7.88
	45°	2	10.3002	8.0822	21.53	8.8380	7.9092	10.50	8.4776	8.0108	5.50
		4	11.4404	8.8089	23.00	9.9739	8.8438	11.33	9.5849	9.0089	6.00
		8	11.9242	9.4557	20.70	10.5618	9.5346	9.72	10.2027	9.6914	5.01
2.0	15°	2	9.3158	7.7821	16.46	8.0143	7.3886	7.80	7.7298	7.4153	4.06
		4	10.3174	8.6288	16.36	9.1081	8.4097	7.66	8.8287	8.4771	3.98
		8	10.4464	8.9674	14.15	9.9214	8.7255	12.05	9.0452	8.7640	3.10
	30°	2	9.3190	6.9857	25.03	7.6402	6.6843	12.51	7.2466	6.7639	6.66
		4	10.4629	7.7902	25.54	8.8974	7.7678	12.69	8.5035	7.9303	6.74
		8	10.8002	8.3738	22.46	9.3861	8.3887	10.62	9.0241	8.5278	5.49
	45°	2	6.5621	6.2080	5.39	6.2145	6.0573	2.52	6.1381	6.0588	1.29
		4	7.1521	6.8149	4.71	6.7778	6.6127	2.43	6.6907	6.6070	1.25
		8	7.5187	7.3201	2.64	7.2119	7.1406	0.98	7.1561	7.1222	0.47

for two-layered cross-ply simply supported plate are given in Table 1(a) and for cylindrical panel in Table 1(b). It can be seen from Table 1 that the results for plate and for positive half cycle of $90°/0°$ cylindrical panel match very well with the respective available solutions. The results of Ref. [9] for negative half cycle do not match with the present results for $90°/0°$ panel rather they match with positive half cycle of $0°/90°$ panel. There appears to be a typographical error in Ref. [9].

Table 5
Non-dimensional positive and negative half cycle frequencies of cross-ply $(0°/90°)_{N/2}$ bimodular laminated SCSC cylindrical panels ($b/h = 10$, Material 1)

L/b	N	$r/h = 20$			$r/h = 50$			$r/h = 100$		
		Ω_1	Ω_2	% diff	Ω_1	Ω_2	% diff	Ω_1	Ω_2	% diff
0.5	2	32.7292	32.8030	−0.22	32.6753	32.7537	−0.23	32.6627	32.7533	−0.27
	4	33.7172	33.6354	0.24	33.6944	33.6314	0.18	33.6884	33.6251	0.18
	8	33.8540	33.7666	0.25	33.8356	33.7772	0.17	33.8304	33.7805	0.14
0.7	2	22.6850	22.4821	0.89	22.6390	22.4769	0.71	22.6282	22.4792	0.65
	4	23.9169	23.7276	0.79	23.9072	23.7359	0.71	23.9041	23.7419	0.67
	8	24.0998	23.9719	0.53	24.0959	23.9838	0.46	24.0939	23.9887	0.43
1.0	2	15.1100	14.6437	3.08	15.0839	14.6465	2.89	15.0789	14.6513	2.83
	4	16.5376	16.2317	1.84	16.5487	16.2462	1.82	16.5508	16.2532	1.79
	8	16.7727	16.5977	1.04	16.7904	16.6151	1.04	16.7938	16.6200	1.03
1.4	2	10.2348	9.4919	7.25	10.2432	9.4936	7.31	10.2476	9.5005	7.29
	4	11.6582	11.2168	3.78	11.6970	11.2352	3.94	11.7063	11.2424	3.96
	8	11.9291	11.7022	1.90	11.9746	11.7237	2.09	11.9851	11.7277	2.14
2.0	2	7.0584	5.9548	15.63	7.1264	5.9619	16.34	7.1457	5.9716	16.43
	4	8.1903	7.5617	7.67	8.2710	7.5867	8.27	8.2906	7.5937	8.40
	8	8.4573	8.1619	3.49	8.5435	8.1896	4.14	8.5639	8.1922	4.34

Table 6
Non-dimensional positive and negative half cycle frequencies of cross-ply $(0°/90°)_{N/2}$ bimodular laminated CSCS cylindrical panels ($b/h = 10$, Material 1)

L/b	N	$r/h = 50$			$r/h = 100$		
		Ω_1	Ω_2	% diff	Ω_1	Ω_2	% diff
0.5	2	28.3702	20.3145	28.39	21.7318	20.8192	4.19
	4	29.7577	21.2174	28.69	23.4795	21.9738	6.41
	8	30.5604	21.7471	28.83	24.5652	22.5066	8.38
0.7	2	27.0713	13.9447	48.48	19.9428	15.0097	24.72
	4	27.9146	15.3093	45.15	20.9763	16.5632	21.03
	8	28.1803	15.9252	43.48	21.3856	17.0980	20.04
1.0	2	26.6889	10.9535	58.95	19.3765	12.4447	35.77
	4	27.3929	12.6503	53.81	20.1813	14.2726	29.27
	8	27.4231	13.3537	51.30	20.3093	14.8374	26.94
1.4	2	26.5917	9.9014	62.76	19.2268	11.6055	39.63
	4	27.2833	11.7605	56.89	20.0043	13.5514	32.25
	8	27.3161	12.5130	54.19	20.0618	14.1372	29.53
2.0	2	26.5775	9.4946	64.27	19.1801	11.3026	41.07
	4	27.2568	11.4288	58.06	19.9797	13.3010	33.42
	8	27.2775	12.2145	55.22	20.0313	13.8960	30.62

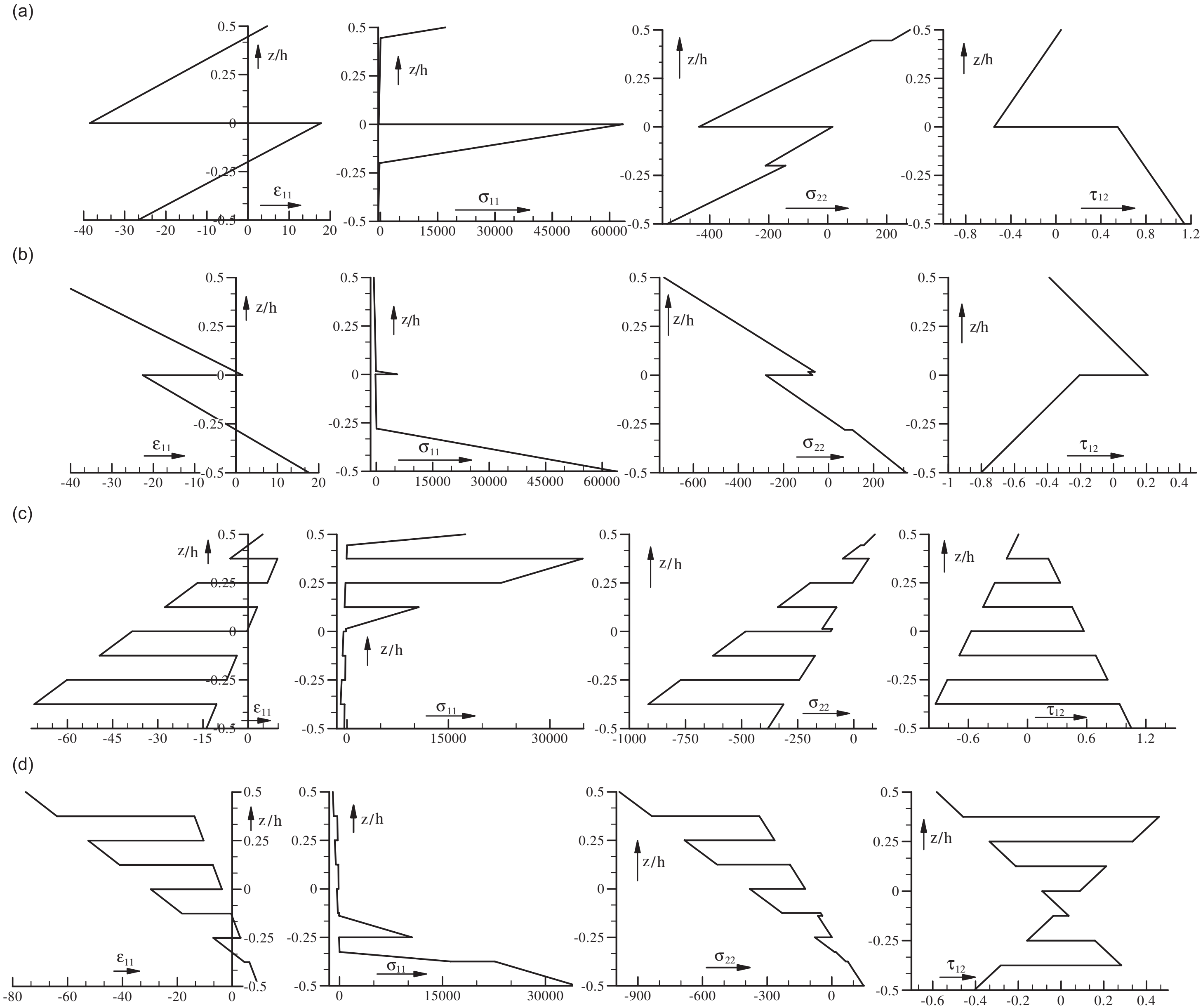

Fig. 6. Variation of modal fiber direction strain (ε_{11}), stresses (σ_{11}, σ_{22}, τ_{12}) along thickness of cross-ply laminated SCSC panels ($r/h = 50$, $b/h = 10$, $L/b = 0.5$, Material 1): (a) 0°/90°, positive half cycle, (b) 0°/90°, negative half cycle, (c) $(0°/90°)_4$, positive half cycle and (d) $(0°/90°)_4$, negative half cycle.

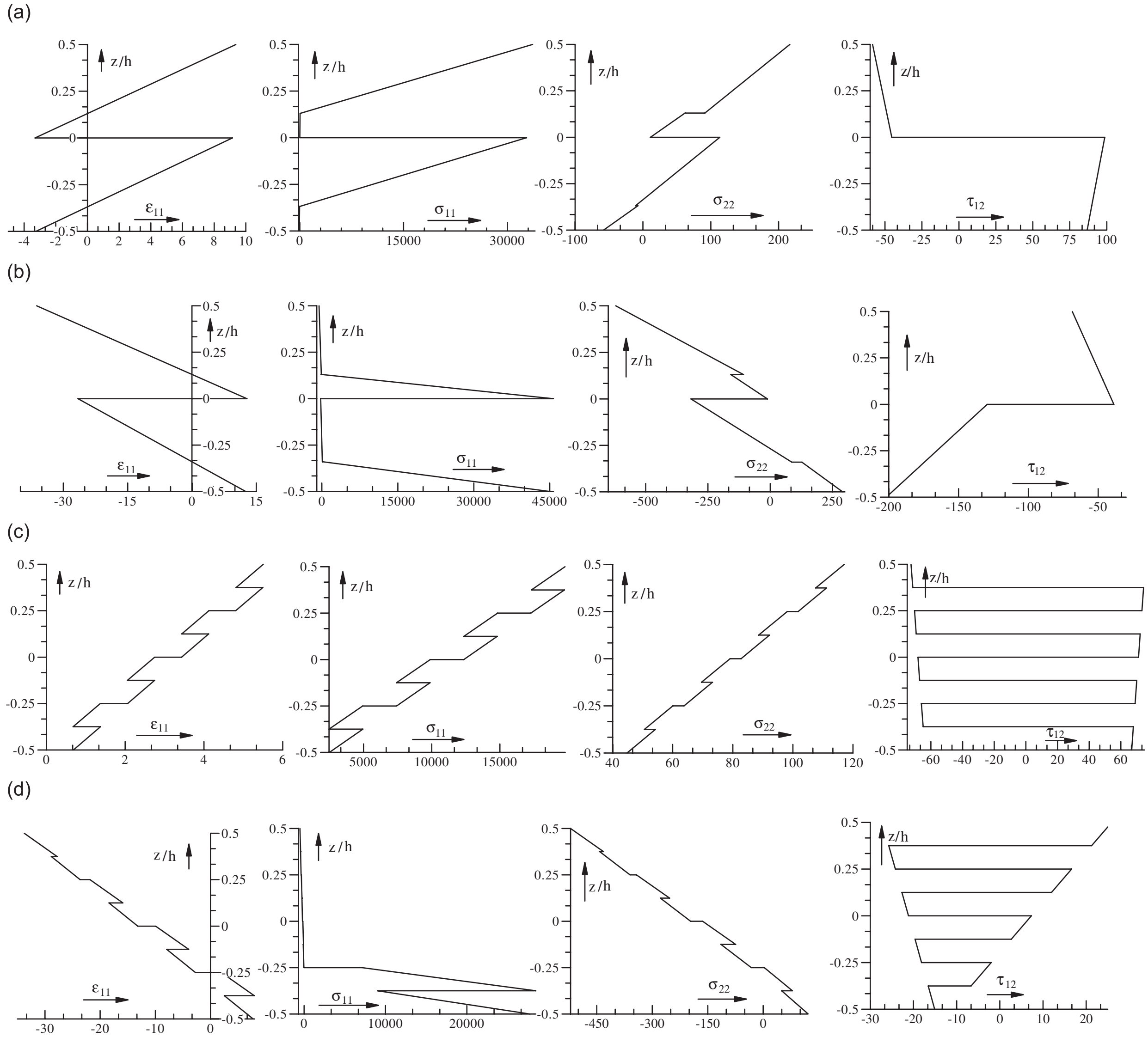

Fig. 7. Variation of modal fiber direction strain (ε_{11}), stresses (σ_{11}, σ_{22}, τ_{12}) along thickness of angle-ply laminated SCSC panels ($r/h = 50$, $b/h = 10$, $L/b = 0.5$, Material 1): (a) $30^\circ/-30^\circ$, positive half cycle, (b) $30^\circ/-30^\circ$, negative half cycle, (c) $(30^\circ/-30^\circ)_4$, positive half cycle and (d) $(30^\circ/-30^\circ)_4$, negative half cycle.

The convergence of the iterative eigenvalue approach for the determination of free vibration frequencies and mode shapes is highlighted in Fig. 4 for CSCS (clamped at $\theta = 0$ and b/r, simply supported at $s = 0$ and L) panels ($r/h = 50$, $L/b = 0.5$, $15^\circ/-15^\circ$) and in Fig. 5 for SSSS (all edges simply supported) panels ($r/h = 100$, $L/b = 1.0$, $(45^\circ/-45^\circ)_4$). The frequency values and corresponding mode shapes for the first five, one intermediate and last two consecutive iterations are presented. It can be inferred from these figures that the rate of convergence is not same for the two cases.

The influence of geometry and lamination scheme on the positive and negative half cycle frequencies of SSSS, CSCS and SCSC bimodular material (Material 1) angle-ply $(\theta/-\theta)_{N/2}$ laminated panels is investigated. The results are depicted in Tables 2–4 for different thickness ratios ($r/h = 20$, 50, 100), ply angles ($\theta = 15^\circ$, 30°, 45°), number of layers ($N = 2$, 4, 8) and aspect ratios ($L/b = 0.5$, 0.7, 1, 1.4, 2). It can be observed from these tables that positive half cycle frequencies are greater than the corresponding negative half cycle frequencies for all the cases except for 15° ply-angle CSCS panels with $L/b = 0.5$ and 0.7. The percentage difference of positive and negative half cycle frequencies ($x = 100\ (\Omega_1 - \Omega_2)/\Omega_1$) decreases as r/h increases. The percentage difference (x) increases with the increase in L/b ratio for SSSS panels with ply-angle $\theta = 15°$ and 30°, for CSCS panels and for 15° ply-angle case of SCSC panels. For other cases, x first increases and then decreases with increase in aspect ratio (L/b). With increase in ply-angle (θ), the percentage difference x

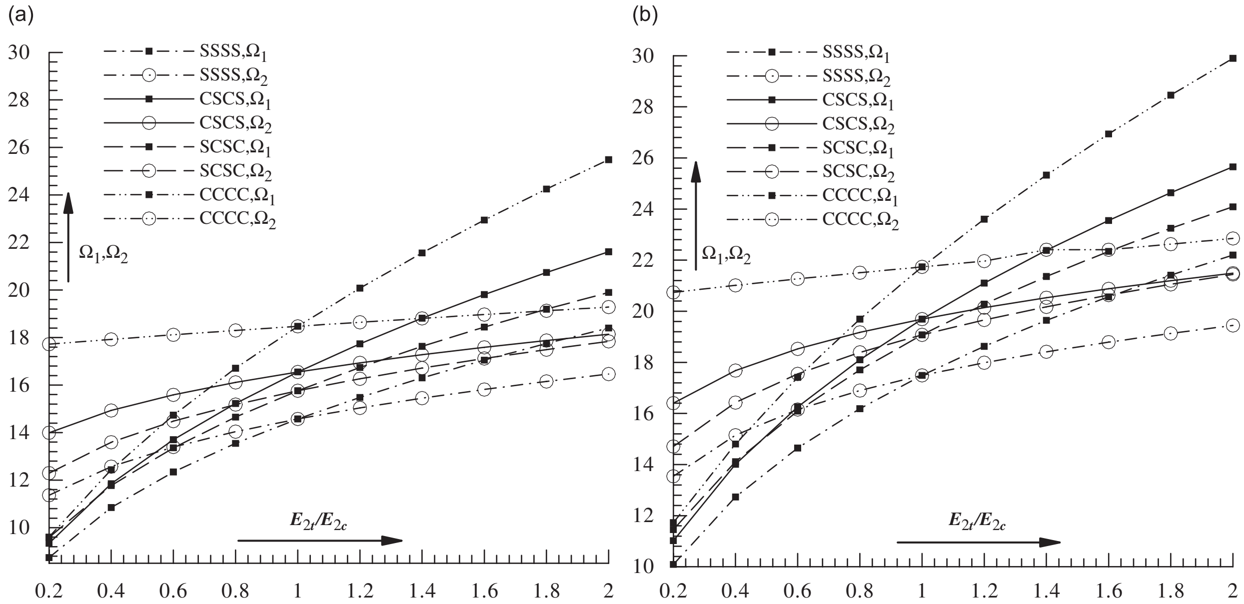

Fig. 8. Variation of positive and negative half cycle frequencies with E_{2t}/E_{2c} of angle-ply panels ($r/h = 20$, $b/h = 10$, $L/b = 1$, Material 2) for different edge conditions: (a) two-layered: 45°/−45° and (b) eight-layered: $(45°/-45°)_4$.

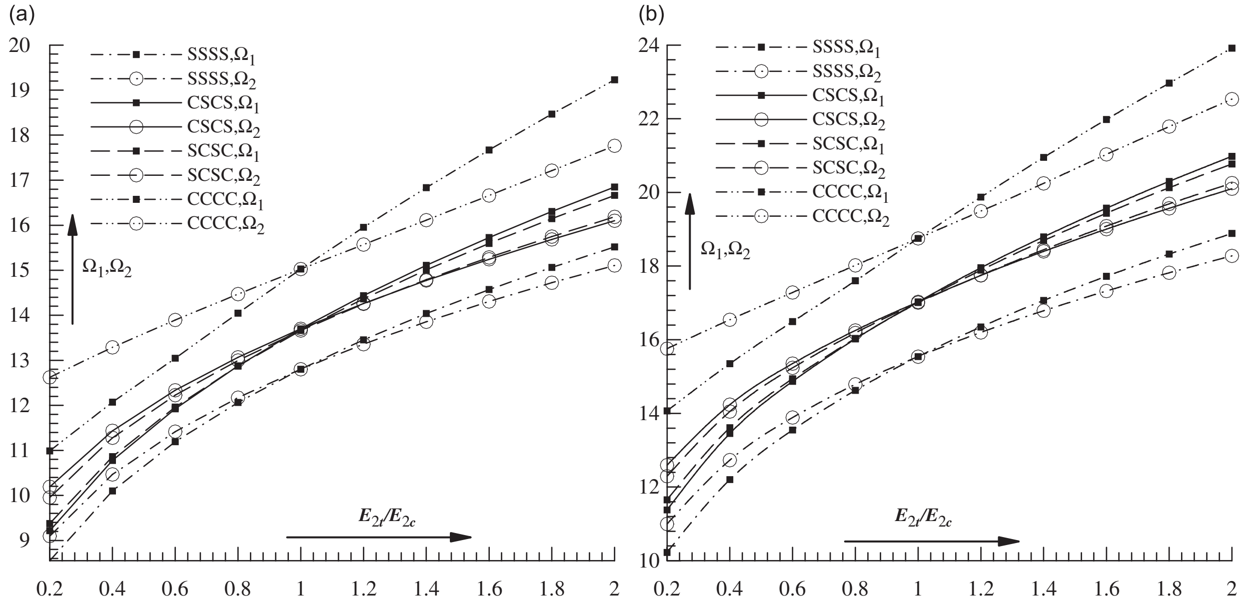

Fig. 9. Variation of positive and negative half cycle frequencies with E_{2t}/E_{2c} of angle-ply panels ($r/h = 100$, $b/h = 10$, $L/b = 1$, Material 2) for different edge conditions: (a) two-layered: 45°/−45° and (b) eight-layered: $(45°/-45°)_4$.

increases except for $L/b = 1.4, 2.0$; $\theta = 45^\circ$ cases of SSSS and SCSC panels. These trends may be attributed to the distribution of fiber direction strain (ε_{11}) deciding the tensile/compressive property assignment. In general, the region corresponding to positive ε_{11} is more for positive half cycle than that for negative half cycle resulting in $\Omega_1 > \Omega_2$.

The positive and negative half cycle frequencies of cross-ply SCSC and CSCS panels are given in Tables 5 and 6, respectively, for different values of r/h, L/b and number of layers. It can be seen from these tables that

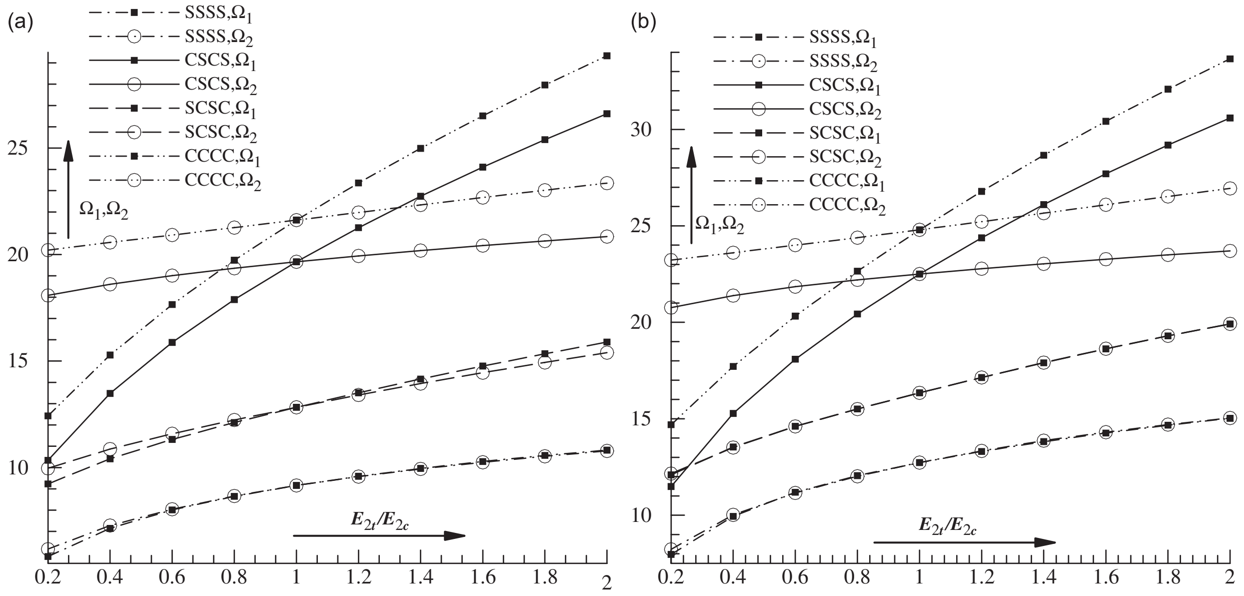

Fig. 10. Variation of positive and negative half cycle frequencies with E_{2t}/E_{2c} of cross-ply panels ($r/h = 20$, $b/h = 10$, $L/b = 1$, Material 2) for different edge conditions: (a) two-layered: 0°/90° and (b) eight-layered: $(0^\circ/90^\circ)_4$.

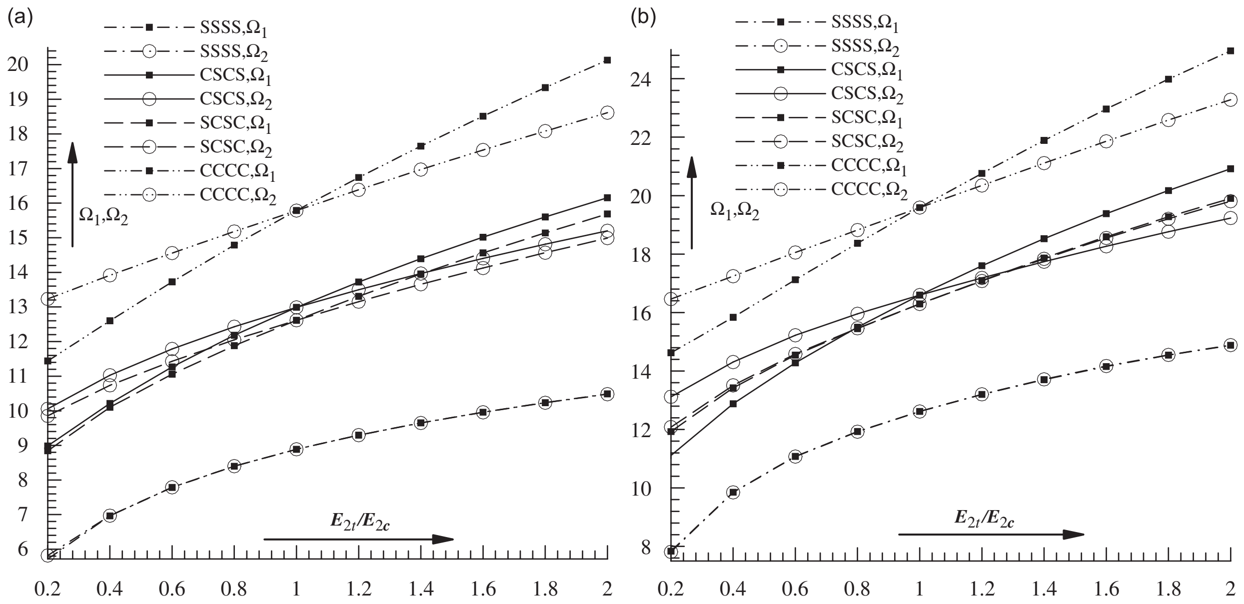

Fig. 11. Variation of positive and negative half cycle frequencies with E_{2t}/E_{2c} of cross-ply panels ($r/h = 100$, $b/h = 10$, $L/b = 1$, Material 2) for different edge conditions: (a) two-layered: 0°/90° (b) eight-layered: $(0^\circ/90^\circ)_4$.

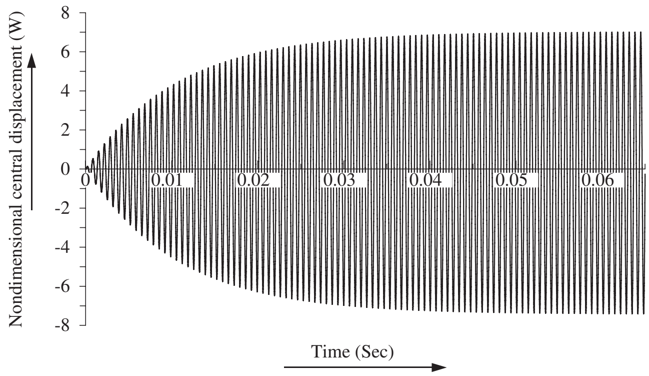

Fig. 12. Non-dimensional central displacement (W) versus time response of eight-layered cross-ply $(0°/90°)_4$ laminated SCSC panel ($r/h = 100$, $L/b = 2.0$, $b/h = 10$, Material 1, $\omega_F/\omega = 1.0$, $\omega = 9376.68$ rad/s).

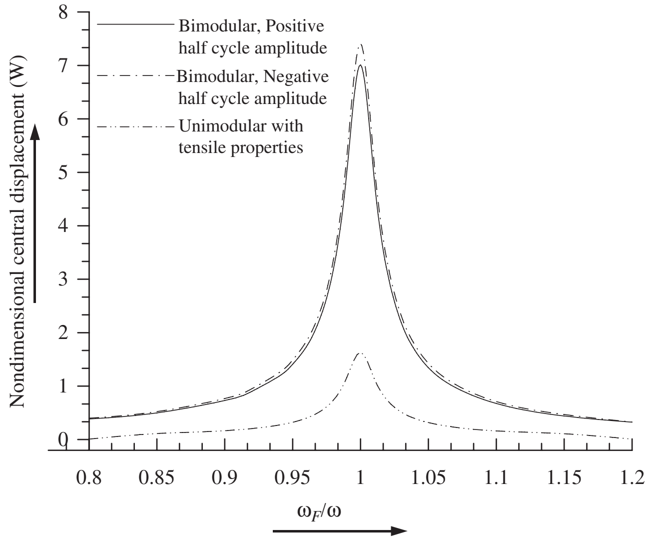

Fig. 13. Frequency response of eight-layered cross-ply $(0°/90°)_4$ laminated SCSC panel ($r/h = 100$, $L/b = 2.0$, $b/h = 10$, Material 1, bimodular: $\omega = 9376.68$ rad/s, unimodular: $\omega = 17110.26$ rad/s).

Ω_1 is greater than the corresponding Ω_2 values except for $L/b = 0.5$ and $N = 2$ in the case of SCSC panels. In general, the percentage difference x increases with increase in L/b and it shows decreasing trend with increase in r/h and number of layers. The modal fiber direction strain (ε_{11}) and stresses (σ_{11}, σ_{22}, σ_{12}) are shown in Fig. 6 for cross-ply and in Fig. 7 for angle-ply SCSC panels for positive and negative half cycles of vibration. It can be seen from these figures that through the thickness distribution of stresses is significantly different for positive and negative half cycles unlike unimodular case wherein the stresses at a particular location in negative half cycle would be of same magnitude but of opposite sign of those corresponding to positive half cycle.

The positive and negative half cycle frequency variation with E_{2t}/E_{2c} ratio of Material 2 of two- and eight-layered cross- and angle-ply cylindrical panels with various edge conditions is shown in Figs. 8–11. It is revealed from these figures that as E_{2t}/E_{2c} increases, Ω_1, Ω_2 values increase. The difference between Ω_1 and Ω_2 decreases as E_{2t}/E_{2c} increases from $E_{2t}/E_{2c} = 0.2$ to 1.0 and it increases as E_{2t}/E_{2c} increases from $E_{2t}/E_{2c} = 1.0$–2.0. This type of behavior is because as E_{2t}/E_{2c} increases (in the range of $E_{2t}/E_{2c} < 1$) the bimodularity ratio (E_{2t}/E_{2c}) decreases and at $E_{2t}/E_{2c} = 1$ it becomes unimodular with positive and negative half cycle frequencies being same. If E_{2t}/E_{2c} increases (in the range of $E_{2t}/E_{2c} > 1$) the bimodularity ratio increases and hence the difference increases. For cross-ply SSSS and SCSC panels, the difference between Ω_1 and Ω_2 is very small as seen from Figs. 10 and 11. The difference between Ω_1 and Ω_2 is greater for panels with straight edges clamped compared to those with straight edges simply supported.

The effect of bimodularity on the steady state response versus forcing frequency relation is studied for eight-layered cross-ply $(0°/90°)_4$ laminated SCSC panel ($r/h = 100$, $L/b = 2.0$, $b/h = 10$, Material 1) subjected to uniformly distributed harmonic force: $q = q_0 \cos(\omega_F t)$. The forcing frequency is varied in the neighborhood of fundamental free vibration average frequency (ω). The proportional damping is taken as: $[C] = 0.02\omega\,[M]$ which corresponds to 0.01 modal damping factor. The typical non-dimensional central displacement $W\,[= w_0 h^3 E_{2c}/(q_0 L^4)]$ versus time response curve for $\omega_F/\omega = 1.0$ is shown in Fig. 12. The steady state response (extracted from time history) versus forcing frequency curves for bimodular panel and unimodular panel with tensile properties are shown in Fig. 13. It can be seen from this figure that there is a significant difference in the frequency response of bimodular and unimodular panels.

6. Conclusion

The free vibration analysis of bimodular laminated composite cylindrical panels is carried out using finite element method based on first order shear deformation theory and the iterative eigenvalue approach. The forced dynamic response is obtained using Newmark's direct time integration scheme. The parametric study is carried out to investigate the effects of panel geometry, lay-up, ply-angle, boundary conditions and bimodularity ratio on the positive and negative half cycle frequencies. The following conclusions can be drawn:

(i) The significant difference between the frequencies of positive and negative half cycles is found depending on the panel parameters.
(ii) The distribution of modal stresses is quite different for positive and negative half cycles unlike unimodular case wherein the stresses at a particular location in negative half cycle would be of same magnitude but of opposite sign of those corresponding to positive half cycle.
(iii) The percentage difference of positive and negative half cycle frequencies decreases as r/h increases.
(iv) As bimodularity ratio increases the positive and negative half cycle frequencies increase.
(v) The frequency response of bimodular and unimodular panels is significantly different.

Acknowledgment

Financial support received from Council of Scientific and Industrial Research (CSIR), New Delhi (India) through Grant No. 22(0401)/06/EMR-II is gratefully acknowledged.

References

[1] J.W. Davis, N.R. Zurkowski, Put the strength and stiffness where you need it, Rept T-STDB (101.05), Reinforced Plastics Division, Minnesota Mining and Manufacturing Company.
[2] Structural Design Guide for Advanced Composite Applications: Material Characterization, vol. 1, second ed., Advanced Composite Division, Air Force Materials Laboratory, 1971.
[3] C.W. Bert, Models for fibrous composites with different properties in tension and compression, *Journal of Engineering Materials and Technology—Transactions of the ASME* 99H (1977) 344–349.
[4] C.W. Bert, J.N. Reddy, W.C. Chao, V.S. Reddy, Vibration of thick rectangular plates of bimodulus composite material, *ASME Journal of Applied Mechanics* 48 (1981) 371–376.
[5] J.L. Doong, L.W. Chen, Vibration of a bimodulus thick plate, *ASME Journal of Vibration, Acoustics, Stress and Reliability in Design* 107 (1985) 92–97.
[6] J.L. Doong, C.P. Fung, Vibration and buckling of bimodulus laminated plates according to a higher order plate theory, *Journal of Sound and Vibration* 125 (1988) 325–339.
[7] B.P. Patel, S.S. Gupta, R. Sarda, Free flexural vibration behavior of bimodular material angle-ply laminated composite plates, *Journal of Sound and Vibration* 286 (2005) 167–186.
[8] B.T. Jzeng, P.D. Lin, L.W. Chen, Dynamic stability of bimodulus thick plates, *Computers & Structures* 45 (1992) 745–753.

[9] C.W. Bert, M. Kumar, Vibration of cylindrical shells of bimodulus composite material, *Journal of Sound and Vibration* 81 (1982) 107–121.
[10] H. Kraus, *Thin Elastic Shells*, Wiley, New York, 1976.
[11] G. Pratap, B.P. Naganarayana, B.R. Somasekhar, Field consistency analysis of the isoparametric eight-noded plate bending element, *Computers & Structures* 29 (1988) 857–863.
[12] V.J. Papazoglou, N.G. Tsouvalis, Mechanical behavior of bimodulus laminated plates, *Composite Structures* 17 (1991) 1–22.